Supplemental Data

Serotonin and G_o Modulate Functional States of Neurons and Muscles Controlling *C. elegans* Egg-Laying Behavior

Stanley I. Shyn, Rex Kerr, and William R. Schafer

Supplemental Experimental Procedures

General Methods and Strains

Nematodes were grown and assayed at 22°C on standard nematode growth medium (NGM) seeded with *E. coli* strain OP50 as a food source.

Construction of *cat-1::iYC2.1*

An ~800 bp derivative of *nde-box::YC2.3* (18× *nde-box* vulval muscle enhancer from *ceh-24* and pSAK-10 backbone originally from A. Fire lab; *YC2.3* from Roger Tsien) with HinDIII, NcoI sticky ends was transplanted to a pPD95.75 backbone containing iYC2.1 (introns added for worm-optimized expression, gift of Jami Dantzker) and then cut again, this time with HinDIII, NotI to replace most of the ~800 bp derivative (a short piece from NotI–NcoI was left in the backbone) with a *cat-1* promoter sequence derived from a *cat-1::gfp* plasmid (gift of Antonio Colavita). The cat-1 promoter was transferred in two pieces: (1) a 2100 bp HinDIII–NsiI restriction fragment from the *gfp* plasmid, and (2) a 214 bp PCR product with NsiI, NotI sticky ends generated from the *gfp* plasmid with PCR primers 5′-CGTGCCTTTCCTTTGAAGTTATTATGCAT-3′ and 5′-ATGCGGCCG CACCTCCTTCTTCCAAGTTTTATTGAATG-3′. The final *cat-1::iYC2.1* construct was microinjected into N2 worms at 25 ng/μl according to the protocol in Mello and Fire [S1]. There was no coinjection marker since transformed worms could be readily identified by fluorescent neurons in the head, midbody, and tail. The extrachromsomal array line used in this study was designated *ljEx65*.

Laser Ablation of VC Neurons

VC neurons 1–6 were ablated in late third-stage/early fourth-stage larvae of *egl-1(n986); nls106(lin-11b::gfp)* worms. Expression of GFP in the developing VC cells was used to identify them prior to the ablation process; cell killing was verified the next day by scoring for the absence of GFP-expressing neurons and neuronal processes.

Optical Imaging of Ca^{2+} Transients

Optical recordings were made from first-day adult hermaphrodite worms immobilized with cyanoacrylate glue on 2% agarose pads dissolved in Dent's saline (140 mM NaCl, 6 mM KCl, 3 mM $CaCl_2$, 1 mM $MgCl_2$, and 5 mM HEPES [pH 7.4]) [S2]. Gluing was dorsal side only for vulval muscle studies but required ventrally, too, in neuronal imaging, to more completely eliminate motion artifact. For drug experiments, serotonin (5-hydroxytryptamine, creatinine sulfate complex, Sigma) was added to the 2% agarose solutions along with a small volume of concentrated NaOH to correct for acidification caused by mM quantities of 5HT. We utilized a W-VIEW beam splitter (Hamamatsu Photonics) to facilitate simultaneous monitoring of cyan and yellow intensities with a single CCD camera (Hamamatsu Orca ER II). In later experiments, this was substituted with a Dual-View Micro Imager (Optical Insights) and Hamamatsu Orca ER CCD camera. Images were acquired with Metavue 4.6 (Universal Imaging) for 1 min at approximately 32–40 Hz (10.8 Hz for neuronal recordings, 20.8 Hz for long N2 vulval muscle recordings) with 4 × 4 binning (8 × 8 for long N2 recordings). Filter/dichroic pairs were: excitation, 420/40; excitation dichroic 455; CFP emission, 480/30; emission dichroic 505; YFP emission, 535/30 (Chroma). Total yellow intensity (Y) of a given muscle was divided by its total cyan intensity (C) to obtain a Y/C ratio that could be used to follow changes in intracellular Ca^{2+}.

Automated Extraction of Fluorescence Intensity Values from Image Series

Image stack analysis for this study was performed much as in [S3], but a menu-driven Java program (Jmalyze) replaced the command line Windows 95 program of the earlier study. A single measurement box/ellipse was defined for each vulval muscle (or neuron), and total yellow and cyan intensities within that region calculated by summing the 12-bit values for each contained pixel prior to ratioing.

Image Data Processing

XY coordinates and total intensity values recorded by Jmalyze to log files were then cut and pasted into templates created in Microsoft Excel to facilitate the evaluation of each ratio trace. Each trace was examined for the presence or absence of Ca^{2+} activity and also for possible motion or tracking artifacts or problems with excessive noise. When enough traces were collected for a given strain and treatment condition, batches of collected imaging data were then processed through MATLAB scripts to normalize baselines and correct for photobleaching and to identify peaks corresponding to Ca^{2+} transients.

Peak Finding

Peak identification was sometimes hampered by excessive noise, and so, while most peak data was retained for calculation of timing and parameters, traces with greater than 10% underdetection of peaks identifiable by eye were discarded. Traces with a few false positives could be manually adjusted in MATLAB to discard individual peak finds deemed unreasonable by eye. Peak identification for vulval muscle and neuronal traces was performed with different MATLAB scripts. In the former case, priority was placed on accurately detecting peaks and avoiding false-positives in the baseline or in noise. A best linear least squares fit was performed for every point in the trace with a nested set of 12 windows of exponentially increasing length (ranging in scale from 5 to 227 frames; each scale larger than the previous by approximately $\sqrt{2}$) centered around the same point. The largest windows were used to estimate linearity of a trace by comparing the goodness of a linear least squares fit for their lengths to the expected goodness of fit given the measured noise. When the probability, p_1, that the error in fit was due to noise dropped below 0.0001, the trace segment in question was declared "nonlinear at scale K." The largest scale (K) where there was still linearity would then set the scale for further analysis at five scales below (K-5) or the shortest scale, by default, if all scales were nonlinear. A peak was defined as at least three consecutive data points where the slope of the fit at that scale was at least 2.0% s^{-1} (unless the smallest scale was being used, in which case this was 1.5% s^{-1}). A peak was extended to include the entire (unbroken) stretch of slopes meeting the given criterion. Failure to detect activity at the K-5th scale would prompt the script to increase the scale by one and repeat this process. Finally, nearby peaks (within 11 frames) were merged into a single peak if they overlapped or if the data points between them fit either peak with a probability, p_2, of at least 10^{-6}. If neither peak accounted for the intervening data points with this stringency, the peaks were kept separate.

Neuronal peak finding prioritized accurate start- and endpoint determination and began by introducing to traces a Gaussian blur of three frames width. A peak was detected every time five out of five frames had a slope of at least 1.0% s^{-1}. To ensure limits were properly chosen, each peak was extended right and left until less stringent slope criteria were failed (still 1.0% s^{-1} to the left, but 0% s^{-1} to the right) on a smaller window of a single frame. Further peak refinement was effected by shrinking a peak to the smallest interval where the endpoints were within expected deviation of noise (1 standard deviation) from the maximum and minimum values detected in the interval defined in the previous step.

Statistical Analysis of Recording Parameters

Statistical comparisons of mean event frequency (vulval muscle Ca^{2+} transients) were performed with the Kolmogorov-Smirnov test

Table S1. Measures of Intermuscle Correlation of Activity

	Fraction Events Correlated	Number of Trace Pairs, $p < 0.05$	Total Number of Trace Pairs	Overall p
N2, no drug	0.232	23	38	8.54×10^{-21}
vm1	0.204	7	12	
vm2	0.260	12	18	
N2, 1.3 mM 5HT	0.547	31*	35	1.99×10^{-36}
vm1	0.555	17	17	
vm2	0.551	8	12	

Fraction events correlated is a mean weighted by the number of events in each muscle/trace pair. p values/quantities were calculated for each pair after assigning random times to the same number of events in each trace to produce a distribution of correlation values arrived at by chance (Monte Carlo estimation, 500 trials). The number of traces assigned p values <0.05 is listed in the second column. An overall probability of having x number of traces with $p < 0.05$ out of y total number of traces (within a given data group) was calculated with Fisher's exact test. Chi-square analysis comparing vm1 versus vm2 for fraction of traces with significant correlations ($p < 0.05$) did not reveal a significant baseline difference. Because the two vulval muscle types occupy different focal planes, we did not study correlation of activity in any vm1-vm2 muscle pairs. While the larger number of events in 5HT traces increased the possibility of correlation by chance, individual pair p values were computed taking this into account. Chi-square analysis (for intergroup comparisons) indicated that the higher fraction of significantly correlated pairs (over the total number of muscle pairs imaged) with 5HT was significantly different from baseline, suggesting the possibility that 5HT enhances electrical coupling between vulval muscles by a mechanism beyond a simple increase in number of Ca^{2+} events.

*$p < 0.01$ (chi square) for overall proportion of 5HT muscle pairs significantly correlated (31/35) versus overall proportion of no drug muscle pairs significantly correlated (23/38).

for goodness of fit (and Bonferroni correction for multiple comparisons, where appropriate). Statistical analysis for our correlation studies is described in the legend to Table S1.

Supplemental References

S1. Mello, C., and Fire, A. (1995). DNA transformation. In *Caenorhabditis elegans*: Modern Biological Analysis of an Organism, Methods in Cell Biology, Volume 48, H.F. Epstein and D.C. Shakes, eds. (San Diego: Academic Press), pp. 451–482.

S2. Avery, L., Raizen, D., and Lockery, S. (1995). Electrophysiological methods. In *Caenorhabditis elegans*: Modern Biological Analysis of an Organism, Methods in Cell Biology, Volume 48, H.F. Epstein and D.C. Shakes, eds. (San Diego: Academic Press), pp. 251–269.

S3. Kerr, R., Lev-Ram, V., Baird, G., Vincent, P., Tsien, R.Y., and Schafer, W.R. (2000). Optical imaging of calcium transients in neurons and pharyngeal muscle of *C. elegans*. Neuron *26*, 583–594.

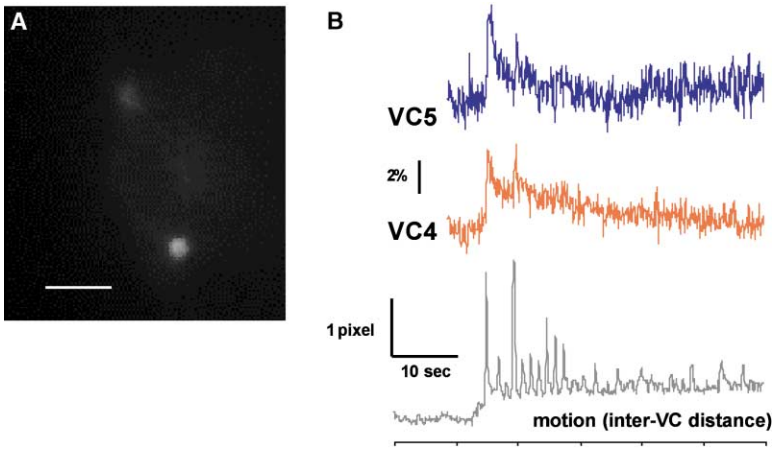

Figure S1. VC Neuronal Imaging with *cat-1::iYC2.1*

(A) Sample field of view showing a pair of VC motorneurons with *cat-1::iYC2.1*. Axons were variably fluorescent. Scale bar is 10 μm.

(B) Ratio traces from simultaneously recorded VC4 and VC5 motorneurons demonstrating correlated activity and consequent vulval muscle twitching (as inferred by coincident increases in inter-VC4,5 distance).

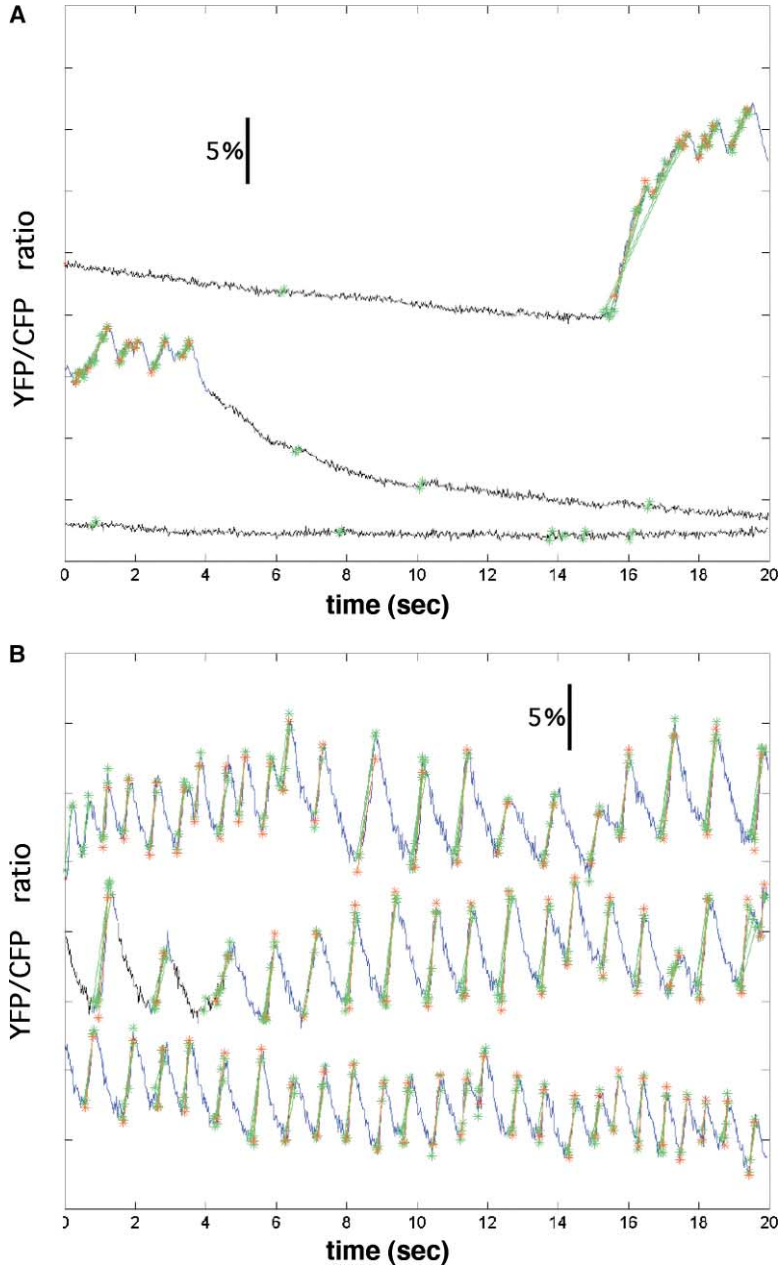

Figure S2. Peak Detection

(A) 1 min N2 [no drug] vulval muscle ratio trace staggered as three segments across 20 s x axis. Ratio trace is in black, with areas of higher activity in blue. Green represents detection of possible activity, with final peak-find calls along the rising phase of Ca^{2+} transients in red, delimited by asterisked endpoints. Y axis represents fractional ratio changes (i.e., 0.05 = 5% increase in Y/C ratio).

(B) 1 min N2 [serotonin] vulval muscle ratio trace. Note that a more extended length of the ratio trace is denoted as a run of higher activity in blue.